Department of Pesticide Regulation

Mary-Ann Warmerdam
Director

M E M O R A N D U M

Arnold Schwarzenegger
Governor

TO: Randy Segawa
Environmental Program Manager I
Environmental Monitoring Branch

FROM: Frank Spurlock, Ph.D. *Original signed by*
Research Scientist III
Environmental Monitoring Branch
916-324-4124

DATE: March 26, 2010

SUBJECT: FUMIGANT TRANSPORT MODELING USING HYDRUS: 3. SELECTION, TEMPERATURE DEPENDENCE AND SENSITIVITY ANALYSIS OF FUMIGANT PHYSICOCHEMICAL PROPERTIES

ABSTRACT

Data sources and estimation procedures for fumigant diffusion coefficients, sorption coefficients, degradation rate constants, and Henry's law constants are critically reviewed. Procedures for estimating temperature dependence are provided. A sensitivity analysis conducted using HYDRUS1D and HYDRUS2/3D shows that the aqueous diffusion coefficient has essentially no effect on fumigant flux under the scenarios studied, and fumigant sorption to soil generally has only a small effect. Among the physicochemical properties, the Henry's law constant, gas phase diffusion coefficient and degradation rate constants have the greatest effect on simulated flux ratios (= total fumigant volatilized/fumigant applied). A simplified evaluation of temperature effects on flux suggests that fumigant property temperature dependence may contribute significantly to diurnal fumigant volatilization dynamics. The analysis suggests that accurate simulation of diurnal fumigant flux dynamics will require consideration of both tarp permeability and fumigant physicochemical property temperature dependence in some cases.

I. INTRODUCTION

The Department of Pesticide Regulation (DPR) is investigating the potential for simulating post-application fumigant volatilization from soils using vadose zone transport modeling. Based on DPR's evaluations of various models, the most promising candidates for simulating fumigant transport in the vadose zone are HYDRUS1D and HYDRUS2/3, depending on the scenario geometry (Johnson, 2008; Gurusinghe, P. 2008; Spurlock, 2009). Previous reports have detailed potential errors in simulated fumigant volatilization arising from use of inaccurate pedotransfer functions to estimate soil hydraulic parameters (Spurlock, 2008), and evaluated HYDRUS1D and HYDRUS2/3D numerical algorithms for both the gas phase diffusion/sorption process within soil, and first-order mass transfer surface volatilization process at the soil surface (Spurlock, 2009). This memorandum continues DPR's investigation of HYDRUS modeling, providing theoretical background, sensitivity analysis, and recommended calculation/estimation

procedures for parameterizing fumigant physicochemical properties. The primary focus is on specific properties required to simulate transport using the HYDRUS family of vadose zone models (Šimůnek et al., 2006; Šimůnek et al. 2009). HYDRUS input variables are:

D_g – gas phase diffusion coefficient ($L^2\ T^{-1}$)
D_w – aqueous phase diffusion coefficient ($L^2\ T^{-1}$)
K_d – soil/water partition coefficient coefficient (may vary by soil layer) (L^3M^{-1})
K_H – dimensionless Henry's constant (air/water partition coefficient)
$k_{1\text{-}s}$ – first order degradation rate constant for the soil phase (T^{-1})
$k_{1\text{-}w}$ – first order degradation rate constant for the aqueous phase (T^{-1})
$k_{1\text{-}g}$ – first order degradation rate constant for the gas phase (T^{-1})
γ_s – zero order sink/source rate constant for the soil phase ($ML^{-3}T^{-1}$)
γ_g – zero order sink/source rate constant for the gas phase ($ML^{-3}T^{-1}$)
γ_w – zero order sink/source rate constant for the aqueous phase ($ML^{-3}T^{-1}$)

An additional variable required to simulate fumigant volatilization from soil in tarped scenarios is the equivalent boundary layer thickness d (L). That property depends on both fumigant and tarp type, but few data are available for the range of tarp types and fumigants used. Therefore, the sensitivity analysis of fumigant properties did not include d. However, the importance of d relative to other fumigant physicochemical properties in simulating volatilization is evaluated later in this paper for the specific case of 1 mil high density polyethylene (HDPE) tarps.

The soil/water partition coefficient K_d for soil with known organic carbon (OC) content is calculated as:

[1] $$K_d = K_{OC} \times OC$$

where K_{OC} is the soil organic carbon normalized partition coefficient. While HYDRUS allows individual first order degradation coefficients to be specified for the gas, aqueous and solid phases, in practice there is no technique for independent measurement of those rate constants in soil-water systems. Thus, unless stated otherwise, the convention here is to describe fumigant degradation in soil using an overall bulk soil degradation constant k_1. The k_1 applies to total solute in the entire system regardless of phase, and $k_{1\text{-}s} = k_{1\text{-}w} = k_{1\text{-}g} = k_1$. Finally, the zero-order sink-source γ are rarely, if ever, used in simulating fumigant or other agrochemical transport. They are not considered further here. Under these assumptions, five basic physicochemical characteristics are generally required to simulate fumigant transport in the vadose zone using HYDRUS: D_g, D_w, K_{OC}, K_H, and k_1.

II. METHODS

A. Sensitivity Analyses

The objective was to evaluate the relative sensitivity of HYDRUS-modeled fumigant volatilization to fumigant physicochemical properties. Fumigant flux ratio was used to assess fumigant volatilization:

$$[2] \quad flux\ ratio = \frac{total\ mass\ fumigant\ volatilized\ from\ profile}{total\ mass\ fumigant\ applied}$$

Two sensitivity analyses were conducted to evaluate the sensitivity of flux ratio to D_g, D_w, K_{OC}, K_H, and k_1.

1. Global Sensitivity analysis. The first sensitivity analysis evaluated Spearman rank correlations between flux ratio and the five fumigant properties for each of four application scenarios. This analysis was "global" in the sense that within each application scenario, each fumigant property was allowed to independently vary over a range of values reported for six current soil fumigants (Table 1). The global analysis yielded mean sensitivity results over the fumigant property parameter space.

Table 1. Ranges of physical chemical properties used in global sensitivity analysis[A]

property	min	max
K_H (dimensionless)	0.005	0.8
K_{OC} (ml gm OC^{-1})	9	83
k_1 (d^{-1})	0.231 ($t_{1/2}$ ~ 3 d)	0.01155 ($t_{1/2}$ ~ 60 d)
D_g ($cm^2\ d^{-1}$)	4320	11230
D_w ($cm^2\ d^{-1}$)	0.432	1.12

[A] *Ranges based on various literature data or estimates for 1,3-dichloropropene, methyl bromide, chloropicrin, methyl isothiocycnate, carbon disulfide, iodomethane. Data compiled from Footprint Pesticide Properties Database, DPR PESTCHEM database, Ruzo (2006), EPISUITE (U.S. EPA, 2009), SPARC on-line (Hilal et al, 2003a, 2003b) and various degradation rate data sources as cited in Dungan and Yates (2003).*

One thousand six hundred simulations were conducted for each scenario using HYDRUS1D or HYDRUS2/3D. The simulations were conducted under the following general conditions.

- The domain of each variable was taken as the approximate range that had been reported or estimated for the common fumigants chloropicrin, methyl bromide, methyl isothiocyanate (MITC), 1,3-dichloropropene (1,3-D), iodomethane, and carbon disulfide (Table 1).
- For each scenario, the same set of 1600 quintets of physicochemical property values were used. For each quintet, the individual values of the five variables were independently and randomly selected from uniform sampling distributions over each variable's domain (Table 1).
- Four application scenarios were considered:
    - a one-dimensional tarped broadcast application in a sandy loam with uniform initial fumigant concentration over the 30-45 cm depth. A boundary layer depth of 250 cm was used to simulate the presence of a tarp with constant mass transfer resistance. Simulated using HYDRUS1D.
    - a one-dimensional untarped broadcast application with two 0.65cm irrigations otherwise identical to the tarped case above. The irrigations took place mid-day on days 1 and 2. Simulated using HYDRUS1D.
    - a one-dimensional untarped broadcast application with no post-application irrigations. This was otherwise identical to the first tarped scenario described above. Simulated using HYDRUS1D.
    - a two-dimensional tarped subsurface drip (line source) application (Figure 1). The application occurred during the first 12h from a semi-circular emitter (1 cm radius) located at the 20 cm depth. Simulated using HYDRUS2/3D.
- An initial uniform soil/water matric potential of –500 cm was used in each scenario. Soil hydraulic parameters were taken as the mean of the most "reliable" fitted van Genuchten soil hydraulic parameters for sandy loam reported in Spurlock (2008a). The sandy loam textural class was used because the majority of California's field fumigations occur in sandy loam soils (Johnson and Spurlock, 2009). Based on the soil hydraulic parameters, the –500 cm initial matric potential corresponded to an initial (uniform) soil water content of 0.188.
- For both the one- and two-dimensional scenarios, OC content versus. depth data were used in conjunction with K_{OC} to simulate variation of K_d with depth (Eq. 1). The OC data were those reported by Troiano et al. (1993) for San Joaquin Valley Hanford sandy loam.
- Flux ratios were calculated for both 21d post-application and 200 d post-application. The 21 d post-application interval was assumed to be the approximate representative time for essentially "complete" dissipation of applied fumigant under actual use conditions. In a few simulations substantial amounts of fumigant remained in the profile after the 21 d interval, likely due to the wide variable domains. Consequently the 200 d post-application

flux ratios were used as a check of sensitivity based on the 21 d flux ratio data. In all cases, the Spearman rank correlations between 200 d flux ratios were essentially equal to those of the 21 d flux ratios.

2. Local one-at-a-time sensitivity analysis. The second sensitivity analysis was a "local" one-at-a-time (OAT) analysis. For the OAT analysis, a baseline simulation was conducted for each of two scenarios using a single quintet of physicochemical property data. The scenarios were the tarped broadcast and subsurface drip scenario. The base values of each of the five properties were chosen as the approximate log-mean of the range endpoints in Table 1: D_g=7800 cm^2 d^{-1}, D_w =0.78cm^2 d^{-1}, K_{OC}=35, K_H=0.125, k_1=0.099 d^{-1}. This OAT analysis yielded the sensitivity for a theoretical fumigant with those base properties. Two simulations were then conducted for each variable where (a) that variable was assigned a value of 1.01 * the base value and 0.99 * the base value, respectively, and (b) all the remaining variables were held constant at their base value z_{base}. This was repeated for each of the five variables, yielding a total of 1 base + 2*5 perturbations = 11 simulations for each of the two scenarios. Two measures of sensitivity for the different variables were calculated, (a) the partial derivative of flux ratio with regard to the $\log_{10}$ of z_{base}, and the relative sensitivity S_r (White and Chaubey, 2005; You and Yang, 2007):

$$[3] \qquad \frac{\partial(\textit{flux ratio})}{\partial \log_{10}(z_{base})} \cong \frac{(\textit{flux ratio}_1)-(\textit{flux ratio}_2)}{\log_{10} z_1 - \log_{10} z_2} \text{ and}$$

$$S_r = \left| \frac{(\textit{flux ratio}_1)-(\textit{flux ratio}_2)}{z_1 - z_2} \quad \frac{z_{base}}{\textit{flux ratio}_{base}} \right|$$

where z_{base} is the base value of the property of interest (D_g, D_w, K_{OC}, K_H, or k_1) and $\textit{flux ratio}_{base}$ is the simulated flux ratio for all $z = z_{base}$. The subscript 1 refers to the first simulation using z (i.e. z = 1.01 * z_{base}), while the subscript 2 refers to the second simulation using z = 0.99 * z_{base}. The partial derivative of flux ratio with respect to $\log_{10}$ z is the change in flux ratio per order of magnitude change in z where all other variables are held constant and the derivative is evaluated at $z=z_{base}$. Larger values of S_r correspond to greater sensitivity of flux ratio to the property.

III. SENSITIVITY ANALYSES RESULTS

A. Global Sensitivity Analysis

Simulations for each of the four application scenarios used the same 1600 quintets of the fate data D_g, D_w, K_{OC}, K_H and k_1. The mean mass balance error for the tarped broadcast, irrigated untarped broadcast, unirrigated untarped broadcast and subsurface drip simulations was 1.6, 0.6, 0.95, and 4.2 percent, respectively. The maximum mass balance error for those scenarios were 4.3, 1.6, 2.8, and 4.4 percent, respectively. The relative sensitivity of the simulated 21 d flux

ratio to the five fate variables was nearly the same in all four scenarios, and also virtually identical to each scenario's "ultimate volatilization" 200 d simulated flux ratio results (results not shown).

The two variables with the largest effect on simulated flux in the global analysis were K_H and k_1. These two variables had absolute values of rank correlation to flux ratios of 0.55 – 0.75 (Table 2). Based on linear regression of $\log_{10}(K_H)$ and $\log_{10}(k_1)$ on flux ratio (not shown), the $\log_{10}$ of these two variables account for approximately 85 – 92 percent of the variation in flux ratios in the four scenarios. Figure 2 illustrates the interaction of k_1 and K_H with respect to flux ratio for each of the four scenarios simulated. For any given $k_1 - K_H$ pair, it's evident that 1-dimensional flux ratios decrease in the order *no tarp/no irrigation* > *no tarp/irrigation* > *tarp* as expected (Figure 2). In addition, the trade-off between volatility and persistence in dictating emissions is evident in all four scenarios, where the combination of lower volatility and higher persistence yields similar flux ratios as high volatility and low persistence.

Over the variable domains and application scenarios examined, flux ratio was completely insensitive to D_w. This demonstrates the expected minimal contribution of aqueous diffusion as a transport process relative to gas diffusion. The effect of D_g was also relatively small (Table 2, Figure 3). This was largely attributable to the narrow range in D_g used in the sensitivity analysis. As discussed later, gas phase diffusion coefficients vary by only a small amount among fumigants.Although gas phase diffusion is the dominant transport mechanism, the narrow range in fumigant D_g resulted in a small effect of D_g on flux ratio relative to K_H and k_1.

Finally, the Spearman correlations of K_{OC} with flux ratio were low in all cases, ranging from ─0.14 to -0.08 (Table 2). In pairwise $\log(K_{OC})$ versus flux ratio plots, there was no obvious visual relationship between K_{OC} and flux ratio (Figure 3). While the rank correlations are statistically significant, the relationships are very weak. Thus, the statistical significance reflects strong evidence for a weak relationship between K_{OC} and flux ratio.

B. Local OAT Sensitivity Analysis

For most variables, the OAT analysis yielded results very similar to the global sensitivity analysis (Table 3):

- the flux rate was insensitive to D_w
- there was a low sensitivity of flux rate to K_{OC}
- a strong dependence of flux rate to both K_H and the lumped soil degradation rate constant k_1

However, flux ratio displayed a much stronger sensitivity to D_g in the OAT analysis as compared to the global analysis. As previously mentioned, fumigant gas diffusion coefficients span a relatively narrow range, so the low sensitivity to this parameter in the global analysis was largely due to the narrow sampling distribution.

C. Sensitivity Summary

In summary, the sensitivity analyses show:

- that aqueous diffusion coefficients are unimportant for simulating fumigant movement in unsaturated soil-water systems.
- there is a low sensitivity of flux ratio K_{OC} in low OC coarse soils. In part this reflects the relatively low K_{OC}s typical of low molecular weight fumigant molecules.
- the two primary driving variables for HYDRUS-simulated flux ratio are K_H and k_1. These two variables accounted for a large majority of the variation in flux ratio in the global analysis scenarios.
- the sensitivity of flux ratio to D_g was low to moderate in the global analysis, but comparable to that of K_H and k_1 in the OAT analysis. The former result was due to the relatively narrow (but realistic) range of D_g in the global analysis.

IV. FUMIGANT PROPERTIES–PARAMETERIZING HYDRUS

A. Temperature Dependence

Degradation rates, diffusion rates and phase partition equilibria of virtually all chemicals vary with temperature. HYDRUS uses an Arrhenius-type relationship to describe the effect of temperature on chemical properties:

$$[4] \qquad \ln\frac{a}{a_r} = \frac{E_a}{R}\left(\frac{1}{T_r} - \frac{1}{T}\right)$$

where a is the value of the variable at temperature T (K), a_r is the known value of the variable at a reference temperature T_r, R is the universal gas constant and E_a is called the "activation energy." The E_a as used to describe the temperature dependence of fate processes in HYDRUS is not a true activation energy in the thermodynamic sense, but this term is retained here for consistency with the historical use of Eq. 4 and the HYDRUS documentation (Šimůnek et al., 2006; Šimůnek et al. 2009). While basic units of length, time and mass are selected by the HYDRUS user, the constant R is an exception: it's value in units of Joule mol^{-1} K^{-1} is hard-coded in the program (R = 8.314). Consequently, E_a is always entered in HYDRUS in units of Joules mol^{-1}. For any of the temperature dependent processes in HYDRUS described by Eq. [4], E_a may be determined from experimental data measured at different temperatures by linear regression of $\ln(a)$ on T^{-1} (e.g. Figure 4). The fumigant parameters K_H, D_g, D_w and k_1 all increase with temperature, so their associated E_a are positive. As point of reference, an E_a of ~50 kJ mol^{-1}

corresponds to an approximate doubling of the parameter *a* in Eq [4] with each 10° increase in temperature (Figure 5). Yates et al. (2002) report diurnal temperature fluctuations of > 40C immediately under the tarp in a California field fumigation. Based on Figure 5, temperature fluctuations that large correspond to diurnal changes in Henry's law constant of a factor of 4 to 5, and changes in degradation rate of a factor of 10. The OAT analysis indicates that changes of that magnitude can have a large effect on flux ratio (Table 3).

B. Gas Phase Diffusion Coefficient D_g

Fumigants are small low molecular weight molecules. Molecular volume is a primary factor determining aqueous and gas phase diffusion coefficients. Consequently, fumigant diffusion coefficients span a relatively narrow range corresponding to their relatively similar molecular size. There are few, if any, direct measurements of fumigant D_g, but several estimation methods are available (Tucker and Nelken, 1991). Based on widespread applicability to different chemical families and relatively low error rates, two of the best methods for D_g are the empirical Fuller, Schettler and Giddings (FSM) method and the theoretically-based Wilke and Lee (WL) method (Tucker and Nelken, 1991). Across a wide variety of 137 nonionic organic compounds, the mean absolute error was 7.6 percent and 4.3 percent for the FSM and WL methods, respectively (Jarvis and Lugg, 1968, as summarized in Tucker and Nelken, 1991). Given (a) the simple expressions used to correct for tortuosity effects on gas phase diffusion in soils, and (b) the relatively small variation in D_g among fumigants, either method should yield suitable estimates for fumigant D_g. The FSM method is much easier to calculate by hand, but the SPARC online calculator <http://ibmlc2.chem.uga.edu/sparc/>, Hilal (2003a, 2003b) provides WL calculation of D_g and as well as many other physicochemical properties of organic compounds.

In theory, gas phase diffusion coefficients are proportional to $T^{1.5}/\Omega(T)$, where Ω is a complex function of several variables (including temperature) known as the collision integral. Experimental gas phase diffusion coefficients generally display an exponential dependence on temperature, where $D_g \propto T^{\eta}$ and η is in the approximate range of 1.5 to 2 (Tucker and Nelken, 1991; Seager et al., 1963). This range in the exponent η corresponds to D_g E_a of approximately 3700 – 5000 J mol^{-1} as calculated via Eq. 4. This amounts to changes of approximately 20–30 percent in D_g over a 40C temperature range. One advantage of using the WL method as implemented in the SPARC on-line calculator is that the method accounts for the temperature dependence of Ω, so is better able to estimate temperature dependence of D_g than the FSM method. SPARC estimated D_g and E_a for currently registered fumigants are given in Table 4.

C. Aqueous Phase Diffusion Coefficient D_w

Aqueous diffusion coefficients are generally about 4 orders of magnitude smaller than those in air, explaining why the contribution of aqueous diffusion to fumigant transport in unsaturated soils is negligible in most cases. While Tucker and Nelken (1991) recommend the Hayduk and Laudie method, the Othmer-Thakar method used by SPARC is essentially identical. Both

methods account for the temperature dependence of the aqueous phase diffusion coefficient solely through the effect of temperature on water viscosity. Table 5 provides SPARC-estimated D_w and E_a.

D. Diffusion In Agricultural Films (Tarps)—Equivalent Boundary Layer Depth *d*

A common mathematical model for simulating solute volatilization at the soil surface is the boundary layer model of Jury et al. (1983). That model describes the gas phase flux density of a solute volatilizing from the soil surface as a first-order mass transfer through a theoretical stagnant boundary layer of thickness *d*:

$$J = \frac{D_g\ [C_{g,0} - C_{g,d}\ ]}{d}$$

[5]

$$= \frac{D_g}{d} C_{g,0} \quad ; \qquad (C_{g,d} << C_{g,0})$$

In Eq. [5], J = solute flux density (M L^{-2} T^{-1}), $C_{g,0}$ is the solute gas phase concentration at the soil surface (M L^{-3}), $C_{g,d}$ is the solute concentration at the top of the boundary layer, and D_g is the solute gas phase diffusion coefficient as before (M^2 T^{-1}). It's commonly assumed that $C_{g,d} << C_{g,0}$. This boundary layer model is implemented in several vadose zone transport modeling programs, including PRZM 3.12, CHAIN2D, HYDRUS 1D, and HYDRUS 2D/3D. The boundary layer thickness *d* describes overall mass transfer resistance at the soil surface. Larger values of *d* correspond to higher resistance and slower transport across the boundary layer. Jury et al. (1983) suggested d = 0.5 cm is a good estimate for a bare surface. To simulate the effect of tarping on fumigant volatilization from soil, much larger equivalent boundary layer thicknesses are used, with values of *d* ranging up to hundreds of cm (Wang et al., 1998; Wang et al. 1997; Yates et al., 2001).

Papiernik et al. (2001) measured mass transfer coefficients h (L T^{-1}) in the laboratory for various fumigants diffusing through 1 mil HDPE film. Those mass transfer coefficients were determined using Fick's first law as applied to a film of thickness *b* subjected to a concentration gradient across the film:

[6] $$J = -D_e\left(\frac{dC}{dx}\right) = -h\,(C_s - C_r)$$

In Eq. [6], D_e is the effective diffusion coefficient of the fumigant in the film, and C_s and C_r are the fumigant concentrations on the source and receiving sides of the film, respectively. The mass transfer coefficient so obtained is unique for a particular fumigant/tarp combination. An equivalent boundary layer thickness d for modeling purposes may be estimated from laboratory-measured h using Eq. [7]:

$$[7] \qquad d = \frac{D_g}{h}$$

Eq. [7] is obtained by equating h to the effective mass transfer coefficient of the equivalent boundary layer = D_g/d. Several studies have shown that tarp permeabilities to fumigants are highly temperature dependent (Papiernik et al., 2001; Wang et al., 1998). This is a direct result of the increase in fumigant D_e within the tarp material with increasing temperature. Papiernik et al. (2001) measured mass transfer coefficients for the current use fumigants methyl bromide, chloropicrin, *cis*-1,3-D and *trans*-1,3-D at five temperatures between 20C and 40C. The temperature dependence of d calculated using Eq. [7] was linearly related to reciprocal temperature as expected from Eq. [4] (Table 6).

The boundary layer E_a are negative (Table 6), meaning that d decreases with increasing temperature, reflecting increased tarp permeability at higher temperatures. The range of E_a in Table 6 correspond to decreases in d of a factor of approximately 1.4 to 1.8 for every 10C increase in tarp temperature (Figure 5).

One of the current shortcomings of the HYDRUS programs is their inability to account for the temperature dependence of tarp permeabilities. As a consequence, they are unable to properly describe the effects of diurnal temperature variation on flux. There is evidence that this shortcoming may be much less problematic when daily mean or cumulative emissions are the primary modeling objective (Yates et al., 2002). However, the question has not been fully explored. As of this writing, DPR is planning for modifications to both HYDRUS1-D and HYDRUS2/3D to improve the ability of those programs to simulate fumigant volatilization dynamics, including the temperature dependence of the boundary layer thickness.

E. Henry's law constant K_H

Henry's law constant is the air-water partition or distribution coefficient. For most low solubility nonionic organic chemicals, Henry's law constants are independent of concentration. HYDRUS uses the dimensionless Henry's law constant:

$$[8] \qquad K_H = \frac{C_g}{C_w}$$

where units of C_g and C_w are typically mass (or mol) per unit volume (e.g. mg L^{-1}, mol m^3, etc). In different references, other units are used to describe concentration in the aqueous and gas phases. For example, C_g is sometimes expressed in pressure units with C_w in mol L^{-1}, so one often sees Henry's constant in various units such as (Pa m^3 mol^{-1}) or (atm l mol^{-1}). To convert from the dimensional Henry's law constants $K_{H,d}$ found in some references to the dimensionless Henry's law constant K_H:

$$[9] \qquad K_H = \frac{K_{H,d}}{RT}$$

where R is the universal gas constant and T is temperature (K). A convenient compilation of gas constants in a variety of units is <http://en.wikipedia.org/wiki/Gas_constant>.
The situation with K_H contrasts with that of the diffusion coefficients in that (a) K_H are variable among fumigants (Table 7), (b) estimation methods are relatively poor (Dearden and Schuurmann, 2003), and (c) there are numerous experimental data available. Thus, estimation procedures should be considered only as a last resort for new chemicals where no experimental data are available.

Because K_H for nonionic organic chemicals are generally independent of concentration, they are often calculated as the ratio of pure component vapor pressure to water solubility. This is acceptable for poorly soluble chemicals, but may be more error-prone than other experimental methods such as vapor-liquid equilibrium measurements. Median coefficients of variation for pesticide solubility and vapor pressure measurements from different sources of 7 and 40 percent, respectively, have been reported (Spurlock, 2008b). Sources of variation include difficulty in reaching solubility limits and saturated vapor pressure conditions. In contrast, vapor-liquid equilibrium measurements allow both phases to be sampled in the same system, typically at some point below saturation.

A second important point about estimating K_H from solubility and vapor pressure is that the data must be for the same temperature and physical state of the compound. Gas solubilities are typically reported for 1 atmosphere partial pressure of the compound (Schwarzenbach et al., 2003), while vapor pressures for some gaseous compounds may be given for the liquid state. For

example, methyl bromide is a gas at 25C (boiling point = 4C). Horvath (1982, as quoted in MacKay et al. 2006)) report a methyl bromide solubility of 15223 g m^3 at standard temperature and pressure (one atmosphere pressure and 25C). The vapor pressure for liquid methyl bromide at 25C is 217700 Pa (Dreisbach, 1961, as quoted in MacKay et al.). Using these two data, a direct (and incorrect) calculation of K_H yields $K_{H,d}$ = 1359 Pa m^3 mol^{-1} (K_H= 0.55) The actual value for methyl bromide $K_{H,d}$ at 25C is in the range of 600 – 700 Pa m^3 mol^{-1} ($0.24 < K_H < 0.28$) (Mackay et al., 2006). The discrepancy is due to the methyl bromide gas solubility, measured at 1 atmosphere = 101325 Pa. Using this for C_g in Eq. [8] along with the solubility given above yields the "correct" $K_{H,d}$ = 632 Pa m^3 mol^{-1} (K_H = 0.26).

Nonionic organic chemical (NOC) K_H are often calculated from solubility data determined in distilled water, but are known to increase with electrolyte. This is a consequence of "salting out," the reduction in NOC solubility with increasing electrolyte content. Görgényi et al. (2006) evaluated the effect of several inorganic ions on K_H for chloroform, benzene, chlorobenzene and anisole. They reported their results in terms of Setschenow constants commonly used to describe the effect of salinity on K_H:

$$[10] \qquad log_{10} \frac{K_{H,sol}}{K_{H,di}} = k_S \; c$$

where c = salt concentration (M), k_S is the Setschenow constant (L mol^{-1}), $K_{H,sol}$ is the Henry's law constant in the electrolyte solution and $K_{H,di}$ is the Henry's constant in distilled water. Their experimentally determined Setschenow constants ranged from about 0.2 to 0.6, depending on organic solute and inorganic electrolyte. These results indicate that electrolyte concentrations on the order of 0.1M would be required to cause a ~10 percent change in K_H.

Worthington and Wade (2007) measured chloropicrin and MITC K_H in distilled water and 0.1M and 0.2M NaCl solutions. They saw no effect of salinity in the case of chloropicrin, but did see a significant increase due to ionic strength (e.g. mean ± sd = 0.0025 ± 0.00205 in distilled water versus 0.0057 ± 0.00205 in 0.2M NaCl). A 0.2M NaCl solution has very high ionic strength, corresponding to an approximate 40 percent seawater solution. Thus, based on the data of Worthington and Wade (2007), and the results of Görgényi et al. (2006), it is safe to assume that fumigant K_H would not be substantially affected by electrolytes in agriculturally viable soils.

Conceptually, it's easiest to understand the effect of temperature on K_H by considering the effect of temperature at the solubility limit $C_w = S^*$ (mg L^{-1}). Combining Eq. [8] and the ideal gas law:

[11] $$K_H = \frac{p^* MW}{S^* RT}$$

where p^* is the pure solute vapor pressure (Pa), MW is molecular weight (g mol^{-1}), T is temperature (K) and R is the gas constant (8.314 J mol^{-1} K^{-1} = 8.314 Pa m^3 mol^{-1} K^{-1}). It is evident from Eq. [11] that the effect of temperature on K_H results from the temperature dependence of both S^* and p^*.

The best method for determining a fumigant's K_H E_a is by analysis of K_H versus T data. If two data are available, Eq. [4] yields E_a. Alternately linear regression of ln(K_H) on reciprocal T yields a slope = E_a/R. K_H versus T data are often not available. In those cases, the enthalpy of vaporization ΔH_{vap} has been used as an estimate for E_a (U.S. EPA, 2001). This approximation works well in many cases – especially for liquids – because the effect of temperature on solubility is often small relative to vapor pressure (Smith and Harvey, 2007).

The approximation $E_a = \Delta H_{vap}$ essentially assumes that the temperature dependence of K_H is due solely to the dependence of p^* on temperature (Schwarzenbach et al., 2003; Smith and Harvey, 2007). That dependence is described by the Clausius-Clapeyron equation (Klotz and Rosenberg, 2008). This yields (Smith and Harvey, 2007):

[12] $$ln\frac{K_H}{K_{H,r}} \approx ln\frac{p^*}{p_r^*} = \frac{\Delta H_{vap}}{R}\left(\frac{1}{T_r} - \frac{1}{T}\right)$$

In Eq. [12], K_{Hr} is the Henry's law constant at reference T_r (K), K_H is the value at T and ΔH_{vap} is in units of R. Enthalpies of vaporization are positive, so K_H increases with temperature. In reality ΔH_{vap} varies with temperature (Chickos and Acree, 2003), but this effect can generally be ignored if ΔH_{vap} is determined in the approximate temperature range where Eq. [12] will be applied. Comparing Eq. [12] and Eq. [4], it is apparent that the HYDRUS K_H E_a = ΔH_{vap} under the assumption that variation in solubility is much less than that of vapor pressure. Table 8 provides a comparison between ΔH_{vap} and K_H Ea (= $\Delta H_{a/w}$, enthalpy of transfer from water to air) for various chemicals using data compiled by Schwarzenbach et al. (2003). The agreement is excellent for small neutral molecules. It's also evident that ΔH_{vap} tends to underestimate $\Delta H_{a/w}$ (E_a) for polar molecules but overestimates $\Delta H_{a/w}$ for very large molecules (Schwarzenbach et al., 2003). The latter is of little importance for small nonpolar fumigant molecules such as methyl bromide and 1,3-D. However, for polar fumigants such as chloropicrin, it's possible ΔH_{vap} may underestimate K_H E_a. Table 9 provides modeling estimates for K_H E_a derived from ΔH_{vap}.

F. Soil-Water Partition Coefficient K_{OC}

Fumigants are relatively small, low-molecular weight molecules. As a result, they are not highly hydrophobic and they display generally low sorption to soils. Both limited data and estimation methods confirm that fumigant K_{OC}s are typically < 100; nearly all estimates are much lower (Table 10). Direct experimental determination of fumigant K_{OC}s are difficult and prone to error. Early estimation methods for nonionic organic compounds yield approximate estimates of K_{OC} typically based on log-log correlations between K_{OC} and K_{OW} or solubility (Lyman, 1990). Since that time, more accurate fragment contribution methods based solely on structure and/or molecular topology have been developed (Meylan et al., 1992). A convenient estimation freeware is the program KOCWIN. This program is one of several property estimation programs included in EPI Suite (U.S. EPA, 2009), a compilation of estimation models for various physical/chemical properties developed by the U.S. EPA and Syracuse Research Corporation (SRC). EPI Suite also includes an extensive library of organic chemical physical and chemical properties based on the SRC environmental fate database. Given the relatively weak effect of sorption on fumigant flux demonstrated in the sensitivity analyses, K_{OC} estimation methods should be adequate for fumigant modeling purposes.

Temperature dependence data for fumigant soil sorption coefficients are sparse. Typical sorption enthalpies for neutral organic compounds in natural soils generally fall in the range of ±20 kJ mol^{-1} (Borisover and Graber, 1998). Enthalpies in this range correspond to relatively small variations in sorption coefficient with temperature (Figure 4). Given the relatively minor influence of fumigant soil sorption on flux, it is reasonable to ignore the temperature dependence of fumigant sorption unless measured data for a given soil are available.

G. Degradation Rate Constant k_1

In contrast to diffusion and air-water partitioning, the mechanisms of fumigant degradation in soil-water systems are complex and poorly understood. Dungan and Yates (2003) provide a detailed summary of laboratory degradation studies of 1,3-D, MITC, chloropicrin and methyl bromide under a range of conditions, including acclimated and amended soils. Recent data for MeI were appended to their compilation (Table 11). The range of reported half-lives are 0.3 – 38.5 days (1,3-D), 0.05 – 34.7 days (MITC), 0.56 – 57.8 days (MeBr) and 0.03 – 4.5 days (chloropicrin) (Table 11). The studies in the Dungan and Yates (2003) review included a broad range of soil, temperature and moisture conditions. Given (a) the implicit uncertainty in extrapolating from laboratory results to actual field conditions, (b) the inability to estimate field specific degradation rates from either first principles or empirical relationships, and (c) the strong influence that degradation rate has on simulated flux, it is likely that simulations of field results will often require inverse estimation of degradation rates. Consequently, in-field time series measurements of soil gas concentrations should be made for use in estimating the degradation rate coefficient directly, defining the objective function for the optimization, or as a check of estimated degradation coefficients.

While the number of laboratory studies are limited, essentially all indicate a strong temperature dependence for fumigant aerobic soil degradation in soil with k_1 E_a in the approximate range of 44,000 – 65,000 J mol^{-1} (Table 12). These E_a correspond to increases in the lumped degradation rate of a factor of 1.8 to 2.4 for every 10C increase in temperature. As a result, degradation rates may vary by an order of magnitude as a result of large diurnal soil temperature fluctuations in the field. When soil-specific data on temperature dependence are not available (which is often the case), the results in Table 12 may be used as a guide for selecting E_a. Alternately, the temperature dependence may have to be ignored and assumed averaged into the inverse estimate of lumped k_1.

H. Comparison of Tarp Permeability and Fumigant Property Temperature Dependence
Some recent modeling efforts have focused on the temperature dependence of tarp permeabilities to account for observed diurnal flux variations, while ignoring the potential contribution of temperature dependent physicochemical properties such as K_H (e.g. Yates et al., 2002; Cryer and van Wesenbeeck, 2009). To evaluate the relative importance of temperature dependence of fumigant properties and tarp permeability, HYDRUS2/3D simulations of a 2-dimensional HDPE-tarped subsurface line-source fumigant application were conducted. The modeling scenario was identical to that used in the HYDRUS2/3D OAT analysis The permeability data of Paperniek et al. (2001) were used to determine equivalent boundary layer thicknesses d for the HDPE tarp (Table 6). All permutations of K_H, D_g, and d at (a) 20C and (b) 30C were used as inputs to evaluate each variable's relative contribution to change in simulated flux ratio resulting from a 10C increase in temperature *throughout the profile*. This design yielded $2^3 = 8$ simulations for each fumigant. Four fumigant chemicals were studied: methyl bromide, *cis*-1,3-D, *trans*-1,3-D, and chloropicrin. Although degradation rate constants k_1 are highly temperature dependent (Table 12), this variable was not considered in the analysis because degradation rates are highly soil/site dependent (Table 11), and mean degradation rates will likely be fitted from field-measured data for any particular modeling scenario.

A variety of tarp materials are used for field fumigations. Different tarp materials yield different mass transfer coefficients for each fumigant, and within tarp materials there are no production standards for tarp permeability. Consequently, the simulation comparisons (Table 13) between HDPE d and fumigant properties illustrate only general principles. It is evident that the relative effect of fumigant property and tarp permeability are widely variable among fumigants. In the case of methyl bromide, the influence of temperature on flux ratio was attributable to both the temperature dependence of tarp permeability and Henry's law constant, with a much lesser impact of D_g. In contrast, the 1,3-D simulations suggest that changes in simulated flux with temperature are at least partially attributable to the temperature dependence of K_H, with the remaining two variables displaying much lesser influence. Similarly, the effect of K_H temperature dependence was also substantial in the case of chloropicrin, although tarp permeability played a role.

The simulation scenarios above almost certainly over-estimate the importance of fumigant physico-chemical property temperature dependence. In actual field conditions, temperature variations decay with depth (Figure 6), so that temperature-induced fluctuations in D_g and K_H decrease with depth. In contrast, a tarp at the soil surface is exposed to the largest temperature changes. A more realistic analysis will require HYDRUS versions capable of simulating temperature effects on tarp permeability. In any event, it is likely that in at least some cases, accurate simulation of temperature-induced flux dynamics will need to include consideration of D_g and K_H temperature dependence as well as tarp permeability.

V. CONCLUSIONS

- Aqueous phase fumigant diffusion coefficients D_w have very little effect on flux. Fumigant D_w may be estimated using standard methods. Representative values are given in Table 5.

- Fumigant soil sorption coefficients K_{OC} do have a weak effect on flux ratio. However, there are limited fumigant experimental K_{OC} data. Fumigant K_{OC}s estimated from molecular connectivity are provided in Table 10 for current fumigants and, in conjunction with field measured soil organic carbon measurements can be used to estimate K_D. These will suffice as input for HYDRUS simulations in most cases. Temperature dependence data for pesticide K_{OC}/K_D are sparse, but usually indicate a relatively weak effect of temperature on sorption. Given overall modeling uncertainty, field variability in fumigant simulation, the small effect of sorption on flux and relatively low K_D temperature dependence, the K_D E_a can be assigned a value of zero with little consequence to estimated flux ratios.

- Fumigant flux ratios are sensitive to gas phase diffusion coefficients D_g. However, the variation in D_g among fumigants is low and estimation procedures are well-developed. The fumigant D_g E_a are in the range of 3700 – 5000 J mol^{-1} based on the WL estimation method. Suggested values for current use fumigant's D_g and E_a are given in Table 4, and the SPARC program (Hilal et al. 2003a, 2003b) can be used to estimate both the D_g of new fumigants and D_g temperature dependence.

- Henry's law constants K_H have a strong effect on simulated flux ratios, are variable among fumigants, and show strong temperature dependence. Estimation methods are relatively poor, with measured data strongly preferred. In general, experimental K_H determined from vapor-liquid equilibrium measurements are more reliable than those calculated from independent measurements of solubility and vapor pressure. The K_H temperature dependence can be estimated directly from measured K_H versus T data, or from the enthalpy of vaporization ΔH_{vap} as determined from vapor pressure versus T data. Various K_H and K_H E_a for fumigants are given in Tables 7 and 9.

- Fumigant flux ratios are sensitive to first-order degradation rate constants k_1, and experimental data demonstrate that k1 are variable among soils. The k1 cannot be estimated from first principles, and will most likely be treated as fitting parameters in many modeling attempts. Some data are given in Tables 11 and 12. The most reliable inverse estimates of k1 will result when time series field soil gas measurements are used in the objective function as well as flux data, or as a check to ensure model mass balance coincides with reality. Experimental data typically show a strong k1 temperature dependence, with calculated Ea in the range of 44,000 to 65,000 J mol-1.

- In most cases, accurate simulation of diurnal flux dynamics will likely require consideration of temperature effects on tarp permeability, K_H and D_g.

REFERENCES

Boesten, J.J.T.I., L.J.T. Van der Pas, J.H. Smelt, and M. Leistra. 1991. Transformation Rate of Methyl Isothiocyanate and 1,3-dichloropropene in Water-saturated Sandy Subsoils. Neth. J. Agric. Sci. 39: 179–190.

Borisover, M.D. and E.R. Graber. 1998. Organic Compound Sorption Enthalpy and Sorption Mechanisms in Soil Organic Matter. J. Env. Qual. 27:312-317.

Chickos, J.S. and W.E. Acree, Jr. 2003. Enthalpies of Vaporization of Organic and Organometallic Compounds, 1880–2002. J. Phys. Chem. Ref. Data, Vol. 32: 519-878.

Creyer, S.A. and I.J. van Wesenbeeck. 2009. Estimating Field Volatility of Soil Fumigants Using CHAIN_2D: Mitigation Methods and Comparison Against Chloropicrin and 1,3-Dichloropropene Field Observations. Environ. Modeling Assess. in press, published online October 2009.

Dearden JC and G. Schüürmann. 2003. Quantitative Structure-Property Relationships for Predicting Henry's Law Constant from Molecular Structure. Env. Tox. Chem. 22:1755-1770.

Doucette, W.J. 2000. Soil and sediment sorption coefficients. In: Handbook of Property Estimation Methods, Environmental and Health Sciences. R.S. Boethling & D. Mackay (Eds.), Boca Raton, FL: Lewis Publishers (ISBN 1-56670-456-1).

Dungan, R.S. and S.R. Yates. 2003. Degradation of Fumigant Pesticides: 1,3-Dichloropropene, Methyl Isothiocyanate, Chloropicrin, and Methyl Bromide. Vadose Zone J. 2:279-286.
Dungan, R.S., A.M. Ibekwe, and S.R. Yates. 2003. Effect of Propargyl Bromide and 1,3-Dichloropropene on Mcrobial Cmmunities in an Organically Amended Soil. Microbiol. Ecol. 43:75–87.

Dungan, R.S., J. Gan, and S.R. Yates. 2001. Effect of Temperature, Organic Amendment Rate, and Moisture Content on the Degradation of 1,3-Dichloropropene in Soil. Pest Manage. Sci. 57:1107–1113.

Dungan, R.S., J. Gan, and S.R. Yates. 2002. Accelerated Degradation of Methyl Isothiocyanate in Soil. Water Air Soil Pollut. 142:299–310.

Elliot,S. 1989. The Solubilty of Carbon Disulfide Vapor in Natural Aqueous Systems. Atmos. Environ.; 23:1977-80.

Gan, J., and S.R. Yates. 1996. Degradation and Phase Partition of Methyl Iodide in Soil. J. Agric. Food Chem. 44:4001–4008.

Gan, J., S.R. Yates, D. Crowley, and J.O. Becker. 1998a. Acceleration of 1,3-Dichloropropene Degradation by Organic Amendments and Application for Emissions Reduction. J. Environ. Qual. 27:408–414.

Gan, J., S.R. Yates, F.F. Ernst, and W.A. Jury. 2000a. Degradation and Volatilization of the Fumigant Chloropicrin after Soil Treatment. Environ. Qual. 29:1391–1397.

Gan, J., S.R. Yates, M.A. Anderson, W.F. Spencer, F.F. Ernst, M.V. Yates. 1994. Effect of Soil Properties on Degradation of Methyl Bromide in soil. Chemosphere 29:2685–2700.

Gan, J., S.R. Yates, S. Papiernik, and D. Crowley. 1998b. Application of Organic Amendments to Reduce Volatile Pesticides Emissions from Soil. Environ. Sci. Technol. 32:3094–3098.

Geddes, J.D., G.C. Miller, and G.E. Taylor, Jr. 1995. Gas Phase Photolysis of Methyl Isothiocyanate. Environmental Science and Technology 29:2590-2594.

Gerstl, Z., U. Mingelgrin, and B. Yaron. 1977. Behavior of Vapam and Methyl Isothiocyanate in Soils. Soil Sci. Soc. Am. J. 41:545–548.

Görgényi, M., J. Dewulf, H. Van Langenhove and K. Héberger. 2006. Aqueous Salting-Out Effect of Inorganic Cations and Anions on Non-Electrolytes. Chemosphere 65:802-810.

Guo, M. and S. Gao. 2009. Degradation of Methyl Iodide in Soil: Effects of Environmental Factors. J. Env. Qual. 38:513-519.

Gurusinghe, P. 2008. Memorandum to Bruce Johnson on Use of LEACHM Model, LEACHP version to predict volatilization component of a pesticide lost from a field application dated June 9, 2008. Available at: <http://www.cdpr.ca.gov/docs/emon/pubs/ehapreps/analysis_memos/2002_Johnson.pdf>.

Hilal, S.H., S.W. Karickhoff and L.A. Carreira. 2003a. Prediction of Chemical Reactivity Parameters and Physical Properties of Organic Compounds from Molecular Structure using SPARC. USEPA publication 600/R-03/030. Available at: <http://www.epa.gov/athens/publications/reports/EPA_600_R03_030.pdf>.

Hilal, S.H., S.W. Karickhoff and L.A. Carreira. 2003b. Verification and Validation of the SPARC Model. USEPA publication 600/R-03/033. Available at: <http://www.epa.gov/athens/publications/reports/EPA_600_R03_033.pdf>.

Horvath, A.L. 1982. Halogenated Hydrocarbons: Solubility-Miscibility with Water. Marcel Dekker, NY, NY.

Jarvis, M. W. and G.A. Lugg. 1968. The Calculation of Diffusion Coefficients of Vapors of Liquids into Air, Report 318 - Australian Defense Scientific Service, p.33; Alexandria, Virginia.

Johnson, B. 2008. Dow Agrosciences-CHAIN2D Review. November 17, 2008 memorandum to J. Sanders. Available at: <http://www.cdpr.ca.gov/docs/emon/pubs/ehapreps/analysis_memos/2094_sanders.pdf>.

Johnson, B. and F. Spurlock. 2009. Dominant Soil Types Associated with Fumigant Applications in Ozone Nonatainment Areas. January 3, 2009 memorandum to R. Segawa. Available at: <http://www.cdpr.ca.gov/docs/emon/pubs/ehapreps/eh4342.pdf>.

Kim, J., S.K. Papiernik, W.J. Farmer, J. Gan and S.R. Yates. 2003. Effect of Formulation on the Behavior of 1,3-Dichloropropene in Soil. J. Env. Qual. 32:2223–2229.

Kresic, N. 2007. Hydrogeology and Groundwater Modeling. 2nd edition. CRC Press, Boca Raton FL

Klotz, I.M. and R.H. Rosenberg. 2008. Chemical Thermodynamics: Basic Concepts and Methods. 7th edition. John Wiley and Sons, NY, NY.

Luo, Y. and X. Yang. 2007. A Multimedia Environmental Model of Chemical Distribution: Fate, Transport, and Uncertainty Analysis. Chemosphere 66(8):1396-1407.

Lyman, W.J.: 1990, 'Adsorption Coefficient for Soils and Sediments', Chapter 4, Handbook of Chemical Property Estimation Methods, Third Edition, Lyman, Rheel, and Rosenblatt, Eds., American Chemical Society, Washington, D.C.

Mackay, D., W. Y. Shiu, K. Ma, S. C. Lee. 2006. Physical-Chemical Properties and Environmental Fate for Organic Chemicals. 4 volumes, 2nd ed., CRC Press, Boca Raton, Fl.

Meylan, W., P.H. Howard and R.S. Boethling. 1992. Molecular Topology/Fragment Contribution Method for Predicting Soil Sorption Coefficients, Environ. Sci. Technol. 26: 1560-7.

Nelson, G.O. 1992. Gas Mixtures, Preparation and Control. CRC Press, Boca Raton FL

Ou, L.-T.,K.-Y.Chung, J.E. Thomas,T.A.Obreza, and D.W.Dickson. 1995. Degradation of 1,3-dichloropropene (1,3-D) in Soils with Different Histories of Field Applications of 1,3-D. J. Nematol. 25: 249–257.

Papiernik, S.K., J. Gan, and S.R. Yates. 2000. Mechanism of Degradation of Methyl Bromide and Propargyl Bromide in Soil. J. Environ. Qual. 29:1322–1328.

Papiernik, S, S.R. Yates and J. Gan. 2001. An Approach for Estimating the Permeability of Agricultural Films. Environ. Sci. Technol. 35:1240-1246.

Papiernik, S. and S.R. Yates. 2002. Effect of Environmental Conditions on the Permeability of High Density Polyethylene Film To Fumigant Vapors. Environ. Sci. Technol. 36:1833-1838.

Ruzo, L.O. 2006. Physical, Chemical and Environmental Properties of Selected Chemical Alternatives for the Pre-plant use of Methyl Bromide as Soil Fumigant. Pest Manag. Sci. 62:99-113.

Seager, S.L., L.R. Geerston and J.C. Giddings. 1963. Temperature Dependence of Gas and Vapor Phase Diffusion Coefficients. J. Chem. Eng. Data 8:168-169.

Schwarzenbach, R.P., P. M. Gschwend and D.M. Imboden. 2003. Environmental Organic Chemistry. 2nd edition. Wiley and Sons, Hoboken NJ.

Šimůnek, J., M. Šejna, H. Saito, M. Sakai, and M. Th. van Genuchten. 2009. The HYDRUS-1D Software Package for Simulating the One-Dimensional Movement of Water, Heat, and Multiple Solutes in Variably-Saturated Media. User Manual version 4.08. Available at: <http://www.pc-progress.com/en/Default.aspx?programs>.

Šimůnek, J., M. Th. van Genuchten and M. Šejna. 2006. The HYDRUS Software Package for Simulating the Two- and Three-Dimensional Movement of Water, Heat, and Multiple Solutes in Variably-Saturated Media. Technical Manual. version 1. Available at: <http://www.pc-progress.com/en/Default.aspx?programs>.

Smelt J H and M Leistra, 1974. Conversion of Metam-sodium to Methyl Isothiocyanate and Basic Data on the Behavior of MITC in Soil. Pestic Sci 5:401-407

Smelt, J.H., W. Teunissen, S.J.H. Crum, and M. Leistra. 1989a. Accelerated Transformation of 1,3-dichloropropene in Loamy Soils. Neth. J. Agric. Sci. 37:173–183.

Smith, F.L. and A.H. Harvey. 2007. Avoid Common Pitfalls When Using Henry's Law. Chemical Engineering Progress 103:33-39.

Spurlock, F. 2008a. Fumigant Transport Modeling Using HYDRUS: Estimation of Soil Hydraulic Parameters Using Pedotransfer Functions. August 14, 2008 memorandum to: R. Segawa. Available at: <http://www.cdpr.ca.gov/docs/emon/pubs/ehapreps/analysis_memos/2066_rosetta.pdf>.

Spurlock, F. 2008b. Distribution and Variance/Covariance Structure of Pesticide Environmental Fate Data. Environ. Toxicol. Chem. 27: 1683-1690.

Spurlock, F. 2009. Fumigant Transport Modeling Using Hydrus: 2. Comparison of Model Simulations to Analytical Solutions of Fick's Second Law of Diffusion. Available at: <http://www.cdpr.ca.gov/docs/emon/pubs/ehapreps/analysis_memos/2163_segawa.pdf>.

Troiano, J., C. Garretson, C. Krauter, J. Brownell, and J. Hutson. 1993. Influence of Amount and Method of Irrigation Water Application on Leaching of Atrazine. J. Environ. Qual. 22: 290-298

U.S. EPA. 2001. FACT SHEET: Correcting the Henry's Law Constant for Soil Temperature. Available at: <http://www.epa.gov/athens/learn2model/part-two/onsite/doc/factsheet.pdf>.

U.S. EPA. 2009. EPISUITE version 4 (Estimation Programs Interface). Available at: <http://www.epa.gov/oppt/exposure/pubs/episuitedl.htm>.

van Dijk, H. 1980. Dissipation Rates in Soil of 1,2-Dichloropropane and 1,3- and 2,3-Dichloropropenes. Pestic. Sci. 11:625–632.

Wang, D., S.R. Yates and W.A. Jury. 1998. Temperature Effect on Methyl Bromide Volatilization: Permeability of Plastic Cover Films. J. Environ. Qual. 27:821-827.

White, K.W. and I. Chaubey. 2005. Sensitivity Analysis, Calibration, and Validation for a Multisite and Multivariable SWAT Model. J. Am. Wat. Res. Assoc. 41(55):1077-1089

Wilhelm, S.N., K. Shepler, L.J. Lawrence, and H. Lee. 1996. Environmental Fate of Chloropicrin. p. 79–93. In J.N. Seiber et al. (ed.) Yates, S.R., D. Wang, F.F. Ernst, and J. Gan. 1997. Ser. 652. American Chemical Society, Washington, DC.

Worthington, E.K. and E.A. Wade. 2007. Henry's Law Coefficients of Chloropicrin and Methyl Isothiocyanate. Atmos. Environ. 41:5510-5515.

Yates, S.R., D. Wang, S. K. Papiernik and J. Gan. 2002. Predicting Pesticide Volatilization from Soils. Environmetrics 13:569-578.

TABLE 2. Spearman rank correlations among 5 fumigant environmental fate variables and simulated 21 day post-application flux ratios. Flux ratios are for four modeling scenarios: (1) tarp broadcast application, (2) tarp subsurface drip, (3) no tarp broadcast, 2 post application irrigations, and (4) no tarp broadcast, no irrigations.

Simple Statistics

Variable	N	Mean	Std Dev	Median	Minimum	Maximum
KH	1600	0.40451	0.22901	0.40650	0.00626	0.79942
K1	1600	0.12034	0.06417	0.11986	0.01167	0.23093
DG	1600	7814	2022	7904	4323	11220
DW	1600	0.77701	0.19951	0.78100	0.43200	1.12300
KOC	1600	45.98273	21.15234	46.72577	9.02958	82.99155
TARP BROADCAST	1600	0.34730	0.17572	0.34192	0.00007	0.79079
TARP SUBSURFACE DRIP	1600	0.43700	0.20417	0.43196	0.00065	0.93117
NOTARP BROADCAST 2IRR	1600	0.40695	0.17430	0.40128	0.00208	0.82820
NOTARP BROADCAST NOIRR	1600	0.49671	0.17840	0.50396	0.00325	0.88533

Spearman Correlation Coefficients, N = 1600
H0: Rho=0

	KH	K1	DG	DW	KOC
KH	1.00000				
K1	r= -0.02955	1.00000			
	p= 0.2375				
DG	-0.05914	0.01689	1.00000		
	0.0180	0.4997			
DW	-0.00986	-0.04151	-0.02311	1.00000	
	0.6934	0.0969	0.3555		
KOC	0.05190	-0.03324	0.02519	-0.03921	1.00000
	0.0379	0.1838	0.3140	0.1170	
21d flux ratios					
TARP BROADCAST	0.68350	-0.58027	0.24210	0.01783	-0.12022
	<.0001	<.0001	<.0001	0.4759	<.0001
TARP SUBSURFACE DRIP	0.64892	-0.63182	0.20570	0.02237	-0.13585
	<.0001	<.0001	<.0001	0.3710	<.0001
NOTARP BROADCAST 2IRR	0.60271	-0.69006	0.21233	0.02301	-0.08391
	<.0001	<.0001	<.0001	0.3577	0.0008
NOTARP BROADCAST NOIRR	0.62478	-0.66225	0.22431	0.02024	-0.08251
	<.0001	<.0001	<.0001	0.4185	0.0010

Table 3. OAT sensitivity analysis results for a theoretical fumigant with properties D_G=7800 cm^2 d^{-1}, D_w =0.78cm^2 d^{-1}, K_{OC}=35, K_H=0.125, k_1=0.099 d^{-1}).

Variable z	$\frac{\partial\,(fluxratio)}{\partial \log_{10}(z)}$	Relative Sensitivity S_r
tarp broadcast application scenario		
21 day simulations		
$\boldsymbol{D_g}$	0.45	0.68
$\boldsymbol{D_w}$	0.00	0.00
$\boldsymbol{k_1}$	-0.43	0.58
$\boldsymbol{K_H}$	0.40	0.61
$\boldsymbol{K_{OC}}$	-0.14	0.26
200 day simulations		
$\boldsymbol{D_g}$	0.45	0.65
$\boldsymbol{D_w}$	0.00	0.00
$\boldsymbol{k_1}$	-0.47	0.66
$\boldsymbol{K_H}$	0.40	0.59
$\boldsymbol{K_{OC}}$	-0.14	0.25
subsurface drip (tarped) scenario		
21 day simulations		
$\boldsymbol{D_g}$	0.45	0.64
$\boldsymbol{D_w}$	0.00	0.00
$\boldsymbol{k_1}$	-0.45	0.65
$\boldsymbol{K_H}$	0.42	0.61
$\boldsymbol{K_{OC}}$	-0.20	0.29
200 day simulations		
$\boldsymbol{D_g}$	0.45	0.61
$\boldsymbol{D_w}$	0.00	0.00
$\boldsymbol{k_1}$	-0.53	0.73
$\boldsymbol{K_H}$	0.42	0.58
$\boldsymbol{K_{OC}}$	-0.19	0.27

Table 4. Estimated fumigant diffusion coefficients in air (cm^2 d^{-1}) and activation energies (J mol^{-1}) at 20C. Data from SPARC, calculated using the Wilke and Lee method (Hilal et al. 2003a, 2003b) unless stated otherwise.

fumigant	$\boldsymbol{D_g}$	$\boldsymbol{E_a}$
1,3-dichloropropene	6886	4560
carbon disulfide	9029[A]	4372[B]
chloropicrin	6515	4566
methyl bromide	10022	4536
methyl iodide	8899	4639
methyl isothiocyanate	8087	4792

[A] Nelsen (1992)

[B] estimated assuming $D_g \propto T^{1.75}$ (see text)

Table 5. Estimated fumigant diffusion coefficients in water ($cm^2\ d^{-1}$) and activation energies ($J\ mol^{-1}$) at 20C. Data from SPARC (Hilal et al. 2003a, 2003b) unless stated otherwise.

fumigant	D_w	E_a
1,3-dichloropropene	0.735	18035
carbon disulfide	0.950[A]	---
chloropicrin	0.707	17920
methyl bromide	0.985	17902
methyl iodide	0.933	17766
methyl isothiocyanate	0.859	17858

[A] as reported in Kresick (2007),Table 6.3

Table 6. Mass transfer coefficients h, gas phase diffusion coefficients D_g, boundary layer depths d and boundary layer activation energies E_a for various fumigants and 1-mil high density polyethelene film.

	Temperature C	h cm hr^{-1} [A]	D_g cm^2 hr^{-1} [B]	d cm [C]	E_a J mol^{-1} (r^2) [D]
methyl bromide					
	20	0.37	417.6	1130	-33760
	25	0.45	432.0	960	0.996
	30	0.62	442.8	714	
	35	0.76	457.2	602	
	40	1.0	471.6	472	
chloropicrin					
	20	0.62	271.4	438	-45780
	25	0.72	280.1	389	0.984
	30	1.2	288.7	241	
	35	1.7	297.4	175	
	40	2.1	306.0	146	
cis-1,3-dichloropropene					
	20	2.0	286.9	144	-33040
	25	2.6	295.9	114	0.947
	30	2.8	304.9	109	
	35	4.9	314.3	64	
	40	5.0	323.6	65	
trans- 1,3-dichloropropene					
	20	3.7	286.9	78	-24820
	25	4.7	295.9	63	0.959
	30	4.8	304.9	64	
	35	6.3	314.3	50	
	40	8.4	323.6	39	

[A] Papiernik et al., 2001

[B] SPARC (Hilal et al. 2003a, 2003b)

[C] calculated using Eq. [7]

[D] calculated from slope E_a/R of d vs reciprocal temperature T^{-1}

Table 7. Selected Henry's law constants from literature.

Fumigant	Estimated	Measured/Calculated from experimental data (25C unless noted)
1,3-dichloropropene	0.069[A], 0.10[B]	0.060[C], 0.045[D] (20C), 0.050[E] (20C), 0.079[E] (30C), 0.055[F]
carbon disulfide	1.23[B]	0.647[G] (20C), 0.785[H], 0.59[I]
chloropicrin	0.18[A], 0.074[B]	0.1[C] , 0.083[J], 0.082[K]
methyl bromide	0.14[A], 0.35[B]	0.24[C], 0.20[L], 0.21[M] (22C), 0.24[N], 0.29[O] (29.4C)
methyl iodide	0.26[A], 0.22[B]	0.21[C], 0.22[L], 0.26[O] (29.4C), 0.18[M] (20C), 0.22[P]
methyl isothiocyanate	0.12[B]	0.01[C], 0.0024[K], 0.0057[F], 0.011[Q] (20C), 0.007[R]

A – SPARC, <http://ibmlc2.chem.uga.edu/sparc/>.

B – HENRYWIN, <http://www.epa.gov/oppt/exposure/pubs/episuitedl.htm>.

C – source unknown, as reported in Ruzo, 2006. 1,3-D data is mean of cis-isomer (0.074) and trans-isomer (0.046).

D – Kim et al., 2003. 1,3-D data is mean of cis-isomer (0.055) and trans-isomer (0.035).

E – Wright et al., 1992, as reported in Mackay et al., 2006, volume 2.

F – FOOTPRINT EU pesticide property database, <http://sitem.herts.ac.uk/aeru/footprint/en/>.

G – De Bruyn et al., 1995, as reported in Staudinger and Roberts, 2001.

H – Yaws et al., 1991, as reported in Mackay et al., 2006, volume 4.

I – Elliot, 1989.

J – Kawamoto and Urano, 1989, as reported in Mackay et al., 2006, volume 4.

K – Worthington and Wade, 2007.

L – Glew and Moelwyn-Hughes, 1953, as reported in Staudinger and Roberts, 2001.

M – Elliot and Rowland, 1993, as reported in Mackay et al., 2006, volume 2.

N – De Bruyn and Saltzman, 1997, as reported in Mackay et al., 2006, volume 2.

O – Swain and Thornton, 1962, as reported in Mackay et al., 2006, volume 2.

P – Hine and Mookerjee, 1975, as reported in Mackay et al., 2006, volume 2.

Q – Geddes et al., 1995.

R – DPR pesticide chemistry database.

Table 8. Comparison of measured enthalpies of vaporization (J mol^{-1}) and actual enthalpies of transfer from aqueous solution to air for selected chemicals (data from Schwarzenbach at el., 2003, page 200).

chemical	ΔH_{vap} (J mol^{-1})	$\Delta H_{a/w} = E_a$ (J mol^{-1})
n-hexane	32	32
n-heptane	37	34
n-octane	41	36
dichlorodifluoromethane	21	27
trichlorofluoromethane	27	23
dichloromethane	29	30
trichloromethane	31	35
trichloroethene	35	37 (mean)
dimethylsulfide	28	30
diethylsulfide	36	37
hexachlorobenzene	76	49
2,5-dichlorobiphenyl	74	47
2,2',5,5',-tetrachlorobiphenyl	81	52
diethyl ether	27	45 (mean)
methyl-t-butyl ether	30	61
methanol	37	45
butanone	35	42

Table 9. Selected fumigant enthalpies of volatilization ΔH_{vap} for use as an estimate of $K_H E_a$. The ΔH_{vap} data were either measured or calculated from vapor pressure versus T data.

Fumigant	Measured/Calculated ΔH_{vap} from data in the approximate range of 5 - 50C (J mol^{-1})
1,3-dichloropropene	*cis*- 26685[A], *trans*- 29190[A]; 32085[B],
carbon disulfide	27522[C], 27944[D], 28500[E]
chloropicrin	39400[F], 39300[E], 39120[G]
methyl bromide	27465[H], 23260[C], 24600[E], 23379[I]
methyl iodide	23992[J], 27970[C], 28200[E]
methyl isothiocyanate	29225[K], 37300[E]

A – Kim et al., 2003.

B – Wright et al., 1992, as reported in Mackay et al., 2006 volume 2.

C – Riddick et al. ,1986, as reported in Mackay et al., 2006 volume 4.

D – Boublik and Aim, 1972, as reported in Mackay et al., volume 4.

E – Chikos and Acree, 2006.

F – Dreisbach, 1961, as reported in Mackay et al., 2006 volume 4.

G – combined data of Baxter et al., 1920, and Stull, 1947, as reported in Mackay et al., 2006 volume 4.

H – De Bruyn and Saltzman, 1997, as reported in Mackay et al., volume 2.

I – Glew and Moelwyn-Hughes, 1953, as reported in Staudinger and Roberts, 2001.

J – Glew and Moelwyn-Hughes, 1953, as reported in Mackay et al., volume 2.

K – Smelt and Liestra, 1974.

Table 10. Selected fumigant organic carbon normalized partition coefficients.

Fumigant	K_{OC}
1,3-dichloropropene	34[A], 26 (mean of 7 values, range 7 - 40)[B], 10.6[C], 56[D], 9.3[E]
carbon disulfide	22[C], 48[D]
chloropicrin	81[A], 36[E], 44[C], 200[D], 62[F]
methyl bromide	39[A], 13.2[C], 10.8[D], 21.9[F]
methyl iodide	28 (mean of 5 values, range 14-61)[G], 13.2[C], 20.4[D]
methyl isothiocyanate	36[A], 10.1[C], 56[D], 9.3[F]

A – Footprint pesticide properties database, <http://www.eu-footprint.org/ppdb.html>.

B – CDPR Pestchem database.

C – KOCWIN module of EPISUITE, U.S. EPA/Syracuse Research Corporation, version 4. Molecular Connectivity Index estimation method (Howard et al. 1992).

D – KOCWIN module of EPISUITE, USEPA/Syracuse Research Corporation, version 4. KOW-KOC linear free energy relation-based estimate (Doucette, 2000).

E – U.S. EPA Chloropicrin Reregistration elegibility decision, 2008, <http://www.epa.gov/oppsrrd1/REDs/chloropicrin-red.pdf>.

F – Syracuse Research Corporation Environmental Fate database, <http://www.syrres.com/what-we-do/efdb.aspx>.

G – CDPR Iodomethane Risk Characterization Document For Inhalation Exposure, Volume III, Environmental Fate, <http://www.cdpr.ca.gov/docs/risk/mei/mei_vol3_ef.pdf>.

Table 11. Summary of laboratory fumigant degradation rate constant and half-life data. All data taken from compilation of Dungan and Yates (2003) except for methyl iodide data.

fumigant	k_1 (d^{-1})	$t_{1/2}$ (day)	description	reference
1,3-dichloropropene	0.037–0.164	18.7–4.2	Four soils at 15C.	van Dijk, 1980
	0.021–0.07	33–9.9	Three soils at 15C.	Smelt et al., 1989a
	0.018–0.019	38.5–36.5	Water-saturated subsoil at 10C.	Leistra et al., 1991
	0.035–0.25	19.8–2.8	Enhanced degradation in previously treated surface and subsurface soils.	Ou et al., 1995
	0.15–1.88	4.6–0.37	Manure-amended soil at 25C.	Gan et al., 1998a
	0.11–2.3	6.3–0.3	Effect of temperature, moisture content, and manure.	Dungan et al., 2001
	0.05–0.30	13.9–2.3	Manure-amended soil at 20C.	Dungan et al., 2003
MITC	0.02–0.19	34.7–3.6	Three soils at 4, 13, or 21C.	Smelt and Leistra, 1974
	0.07–0.21	9.9–3.3	Six soils at 20C, 20% moisture.	Gerstl et al., 1977
	0.011–0.43	64–16	Four soils at 4C.	Boesten et al., 1991
	0.21–13.5	3.4–0.05	Manure-amended soil at 25C.	Gan et al., 1998b
	0.12–2.0	5.8–0.35	Effect of temperature, moisture content, and manure.	Dungan et al., 2002
MeBr	0.012–0.12	57.8–5.8	Four soils at different moisture contents.	Gan et al., 1994
	0.03–0.12	23.1–5.8	Three soils and potting mix at 24C.	Gan and Yates, 1996
	0.06–1.24	11.6–0.56	Manure-amended soil at 25C.	Gan et al., 1998b
	0.015–0.19	46.2–3.6	Two soils at 25C.	Papiernik et al., 2000
chloropicrin	0.15	4.5	Sandy loam soil at 25C.	Wilhelm et al., 1996
	0.16–23.7	4.3–0.03	Effect of temperature and moisture content in three different soils.	Gan et al., 2000a
MeI	0.0102-0.222	3.5-67.9	Effect of temperature and moisture content in three different soils[A]	Gao and Guo, 2009

[A] Calculated MeI degradation rates based on a first-order "availability adjusted" rate model. See Gao and Guo (2009) for details.

Table 12. Degradation rate constant k_1 activation energies E_a (J mol^{-1}) calculated from experimental data (Calculated from Eq. 4 or linear regression of ln(k_1) on reciprocal temperature).

Fumigant	Process	Measured/Calculated from experimental data (25C unless noted)
1,3-dichloropropene	hydrolysis	2 temperatures, *cis*-100200; *trans*-103300[A]
1,3-dichloropropene	hydrolysis	3 temperatures, 99970[B]
1,3-dichloropropene	aerobic soil degradation	1 soil: sandy loam @ 20C, 30C, 40C *cis*- 54700, *trans*- 63200[C]
methyl isothiocyanate	aerobic soil degradation	3 soils: humic sand, loamy sand, loam @ 4C, 12C, 20C. 64300, 52600, 65400, respectively[D].
methyl isothiocyanate	aerobic soil degradation	1 soil: sandy loam @ 20C, 30C, 40C. 64300[E]
chloropicrin	aerobic soil degradation	3 soils: sandy loam, loamy sand, silt loam. 20C, 30C, 40C, 50C. 57500, 62200, 51100, respectively [F]
methyl iodide	aerobic soil degradation	sandy loam: 10C, 20C, 30C, 43700[G]

A – Kim et al., JAFC 2003.
B – McCall, Pest Sci 1987.
C – Dungan et al. (2001).
D – Smelt and Liestra, 1974.
E – Dungan et al. 2003.
F – Gan et al. 2001.
G – Guo and Gao, 2009.

Table 13. Effect of 10C change in temperature (20C → 30C) on simulated 21d flux ratio. Simulated assuming "one at a time" changes in individual variables (K_H, D_G and *d)* and for changes in all variables simultaneously. HYDRUS2/3D simulation scenario was a 2-dimensional HDPE-tarped subsurface line-source fumigant application.

methyl bromide – HDPE										
$K_{H,T}$	K_H [A]	$D_{g,T}$	D_g cm^2 day [B]	boundary layer, d_T	d cm [C]	21d flux ratio	Δ flux ratio K_H 20 →30	Δ flux ratio D_g 20 →30	Δ flux ratio d 20 →30	Δ flux ratio all variables 20 →30
$K_{H,20}$	0.218	$D_{g,20}$	10022	d_{20}	1130	0.293				
$K_{H,30}$	0.295	$D_{g,20}$	10022	d_{20}	1130	0.349	0.056		.	
$K_{H,20}$	0.218	$D_{g,20}$	10022	d_{30}	714	0.355			0.062	
$K_{H,30}$	0.295	$D_{g,20}$	10022	d_{30}	714	0.414	0.059		0.065	
$K_{H,20}$	0.218	$D_{g,30}$	10657	d_{20}	1130	0.306		0.012		
$K_{H,30}$	0.295	$D_{g,30}$	10657	d_{20}	1130	0.362	0.057	0.013		
$K_{H,20}$	0.218	$D_{g,30}$	10657	d_{30}	714	0.368		0.013	0.062	
$K_{H,30}$	0.295	$D_{g,30}$	10657	d_{30}	714	0.428	0.060	0.014	0.066	0.134
						Mean	**0.058**	**0.013**	**0.064**	
***cis*-1,3-dichloropropene - HDPE**										
$K_{H,20}$	5.00E-02	$D_{g,20}$	6886	d_{20}	144	0.156				
$K_{H,30}$	7.86E-02	$D_{g,20}$	6886	d_{20}	144	0.228	0.072		.	
$K_{H,20}$	5.00E-02	$D_{g,20}$	6886	d_{30}	109	0.166			0.010	
$K_{H,30}$	7.86E-02	$D_{g,20}$	6886	d_{30}	109	0.239	0.073		0.011	
$K_{H,20}$	5.00E-02	$D_{g,30}$	7325	d_{20}	144	0.165		0.009		
$K_{H,30}$	7.86E-02	$D_{g,30}$	7325	d_{20}	144	0.239	0.074	0.011		
$K_{H,20}$	5.00E-02	$D_{g,30}$	7325	d_{30}	109	0.175		0.010	0.010	
$K_{H,30}$	7.86E-02	$D_{g,30}$	7325	d_{30}	109	0.250	0.075	0.011	0.012	0.094
						Mean	**0.073**	**0.010**	**0.011**	
***trans*-1,3-dichloropropene – HDPE**										
$K_{H,20}$	5.00E-02	$D_{g,20}$	6886	d_{20}	78	0.176				
$K_{H,30}$	7.86E-02	$D_{g,20}$	6886	d_{20}	78	0.250	0.075		.	
$K_{H,20}$	5.00E-02	$D_{g,20}$	6886	d_{30}	64	0.180			0.005	
$K_{H,30}$	7.86E-02	$D_{g,20}$	6886	d_{30}	64	0.256	0.075		0.005	
$K_{H,20}$	5.00E-02	$D_{g,30}$	7325	d_{20}	78	0.185		0.010		
$K_{H,30}$	7.86E-02	$D_{g,30}$	7325	d_{20}	78	0.261	0.076	0.011		
$K_{H,20}$	5.00E-02	$D_{g,30}$	7325	d_{30}	64	0.190		0.010	0.005	
$K_{H,30}$	7.86E-02	$D_{g,30}$	7325	d_{30}	64	0.267	0.076	0.011	0.005	0.091
						Mean	**0.076**	**0.011**	**0.005**	

(continued)

***chloropicrin* – HDPE**										
$K_{H,T}$	K_H [A]	$D_{g,T}$	D_g cm^2 day [B]	boundary layer, d_T	d cm [C]	21d flux ratio	Δ flux ratio K_H 20 →30	Δ flux ratio D_g 20 →30	Δ flux ratio d 20 →30	Δ flux ratio all variables 20 →30
$K_{H,20}$	6.26E-02	$D_{g,20}$	6515	d_{20}	438	0.123				
$K_{H,30}$	1.07E-01	$D_{g,20}$	6515	d_{20}	438	0.198	0.076		.	
$K_{H,20}$	6.26E-02	$D_{g,20}$	6515	d_{30}	241	0.157			0.034	
$K_{H,30}$	1.07E-01	$D_{g,20}$	6515	d_{30}	241	0.242	0.085		0.044	
$K_{H,20}$	6.26E-02	$D_{g,30}$	6931	d_{20}	438	0.131		0.008		
$K_{H,30}$	1.07E-01	$D_{g,30}$	6931	d_{20}	438	0.209	0.078	0.010		
$K_{H,20}$	6.26E-02	$D_{g,30}$	6931	d_{30}	241	0.166		0.009	0.035	
$K_{H,30}$	1.07E-01	$D_{g,30}$	6931	d_{30}	241	0.253	0.087	0.011	0.045	0.131
						Mean	**0.082**	**0.010**	**0.039**	

A methyl bromide K_H from data of Glew and Moelwyn-Hughes (1953) as reported in Mackay et al.,2006, volume 2; *cis*- and *trans*- 1,3-dichloropropene K_H are average for both isomers (Wright et al., 1992, as reported in Mackay et al., 2006, volume 2); chloropicrin $K_{H,20}$ from Kawamoto and Urano, 1989, as reported in Mackay et al., 2006, version 4, chloropicrin $K_{H,30}$ calculated using Eq. 4 and mean ΔH_{vap} (Table 9).

B D_g from SPARC (Hilal et al. 2003a, 2003b) (see Table 4).

C d calculated using Eq. [7] and mass transfer data of Papiernik et al., (2001).

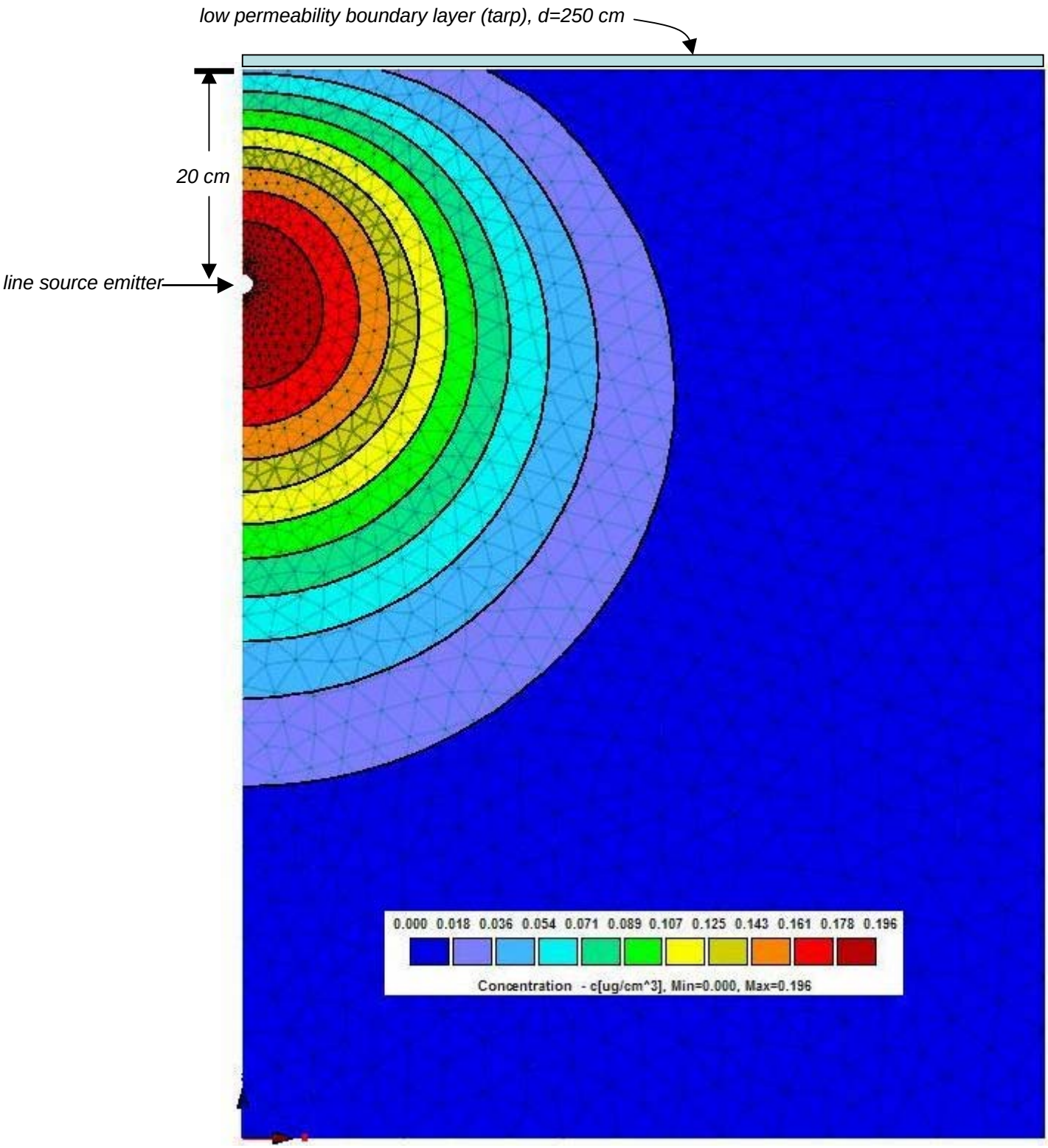

Figure 1. HYDRUS2/3D line source “drip” modeling domain used in sensitivity analysis. Color contours show relative fumigant concentration at time=1day

Figure 2. Flux ratio contour plots on k_1, K_H from global sensitivity analysis.

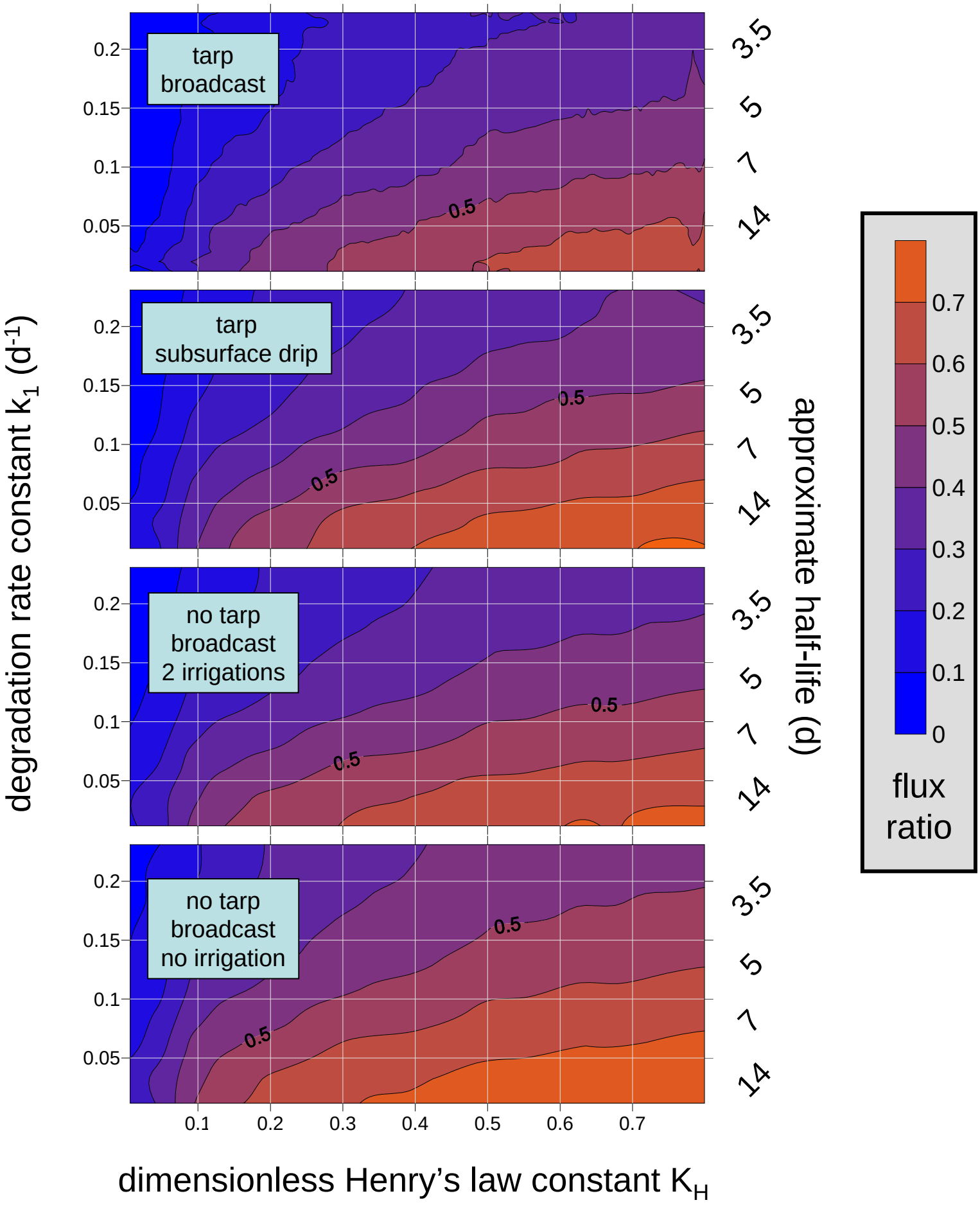

Figure 3. Matrix plot of data ranks from global sensitivity analysis. Fumigant physicochemical properties and flux ratios (FR) for four fumigation modeling scenarios: (a) drip, (b) no tarp, no irrigation broadcast, (c) no tarp, 2 irrigations broadcast, and (d) tarped broadcast.

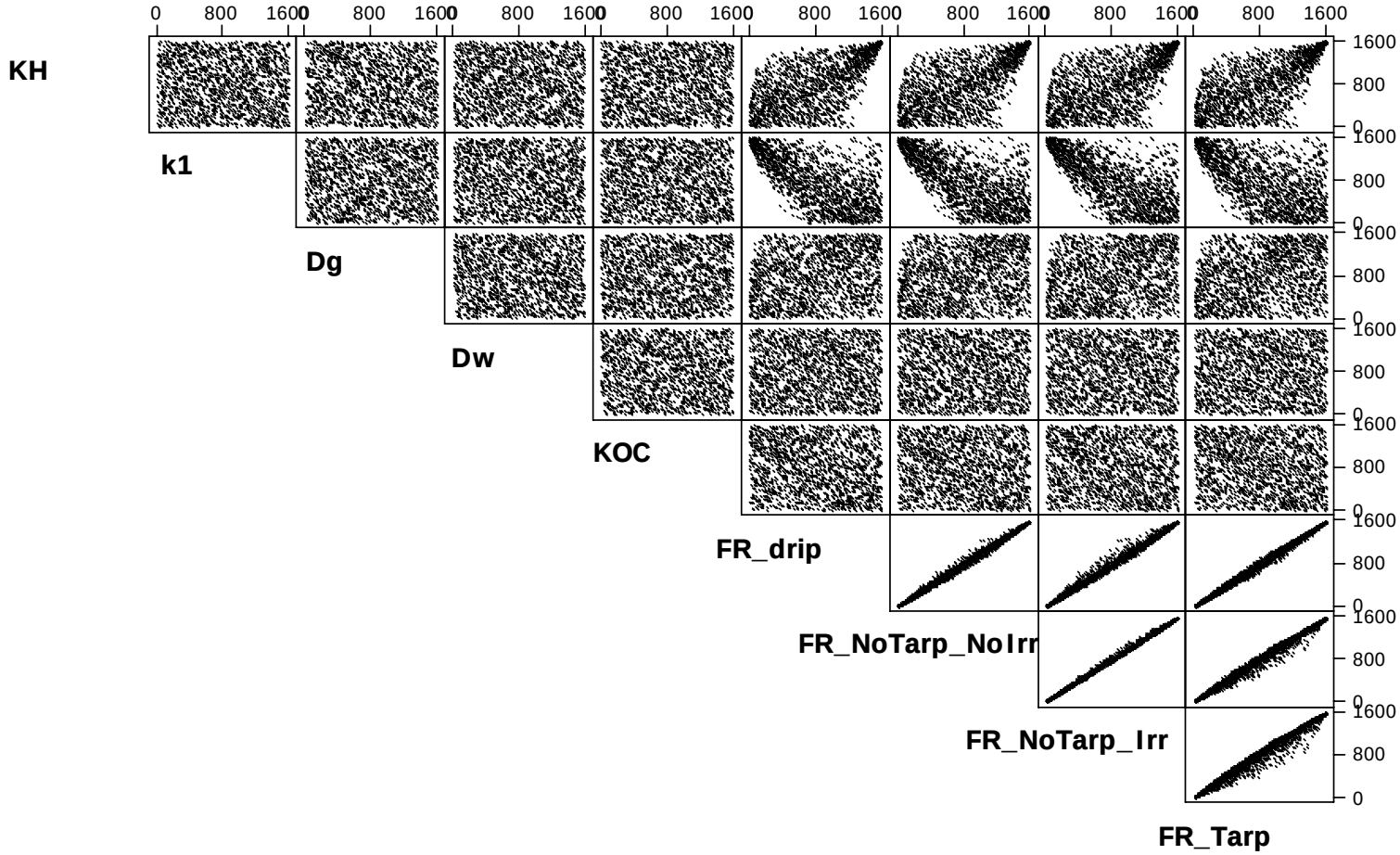

Figure 4. Arrhenius plot of first order degradation rate constant for lumped degradation of chloropicrin in Arlington sandy loam illustrating estimation of activation energy (data from Gan et al., 2000a).

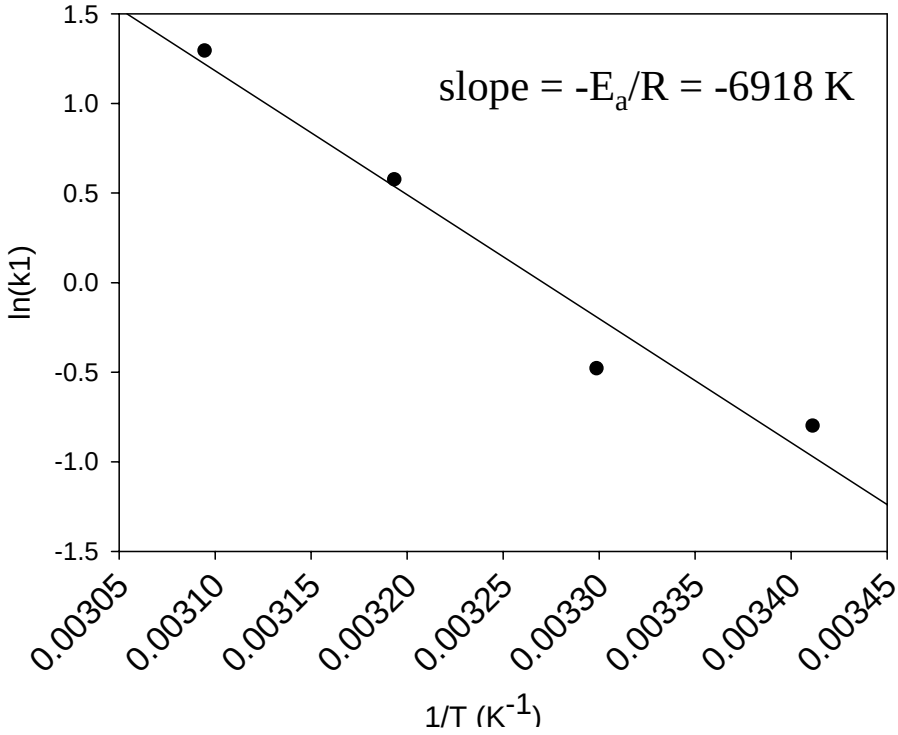

Figure 5. Effect of activation energy E_a on temperature dependence of properties as calculated using Eq. [4]. The Y-axis shows relative increase in a particular property with each 10 degree increase in temperature. The X-axis shows approximate range of activation energy for various properties as estimated from various sources cited in this paper.

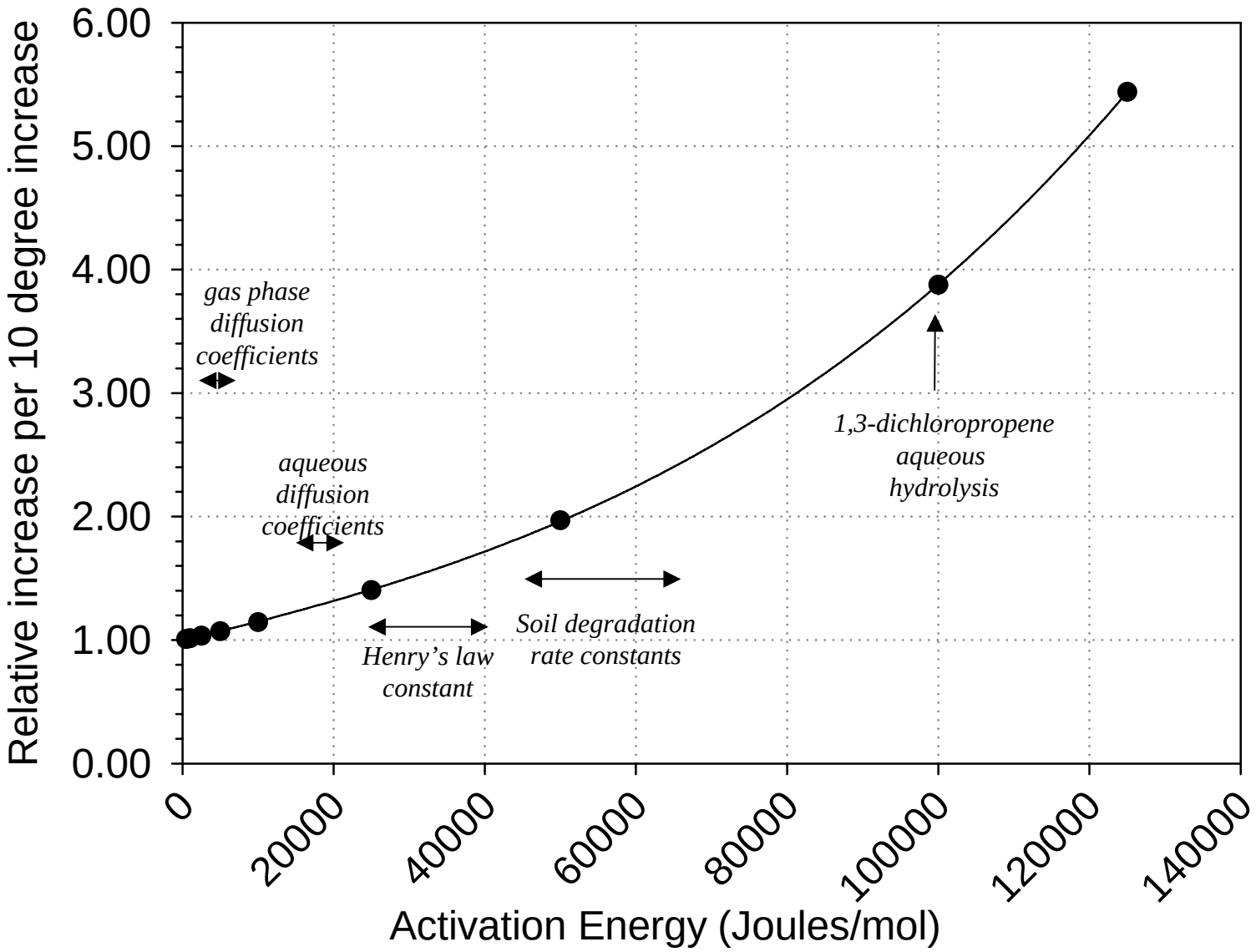

Figure 6. Illustrative example of diurnal temperature variation at different soil depths. Based on HYDRUS simulations using default thermal conductivity and heat capacity data for sandy soil.